Alteration of long and short-term hematopoietic stem cell ratio causes myeloid-biased hematopoiesis

Running title; Self-renewal heterogeneity causes myeloid skewing

Katsuyuki Nishi[1,2], Taro Sakamaki[1,2], Akiomi Nagasaka[1,2], Kevin S. Kao[3], Kay Sadaoka[1,2], Masahide Asano[4], Nobuyuki Yamamoto[5], Akifumi Takaori-Kondo[6], Masanori Miyanishi[1,2] *

[1]Hematopoietic Stem Cell Biology and Medical Innovation (HSCBMI), Department of Pediatrics, Kobe University Graduate School of Medicine, Kobe, Hyogo 650-0047, Japan

[2]RIKEN Center for Biosystems Dynamics Research, Kobe, Hyogo 650-0047, Japan

[3]Weill Cornell, Rockefeller, Sloan-Kettering, Tri-Institutional MD-PhD Program, New York, NY

[4]Institute of Laboratory Animals, Kyoto University Graduate School of Medicine, Kyoto, Kyoto, 606-8501, Japan.

[5]Department of Pediatrics, Kobe University Graduate School of Medicine, Kobe, Hyogo 650-0017, Japan

[6]Department of Hematology and Oncology, Kyoto University Graduate School of Medicine, Kyoto, Kyoto 606-8507, Japan

*Correspondence: Masanori Miyanishi, M.D, Ph.D.

Hematopoietic Stem Cell Biology and Medical Innovation (HSCBMI), Department of Pediatrics, Kobe University Graduate School of Medicine, Kobe, Hyogo 650-0047, Japan

E-mail: miya75@med.kobe-u.ac.jp

Phone: 078-304-6037

FAX: 078-304-6100

Abstract

Myeloid-biased hematopoiesis is a well-known age-related alteration. Several possibilities, including myeloid-biased hematopoietic stem cell (HSC) clones, may explain this. However, the precise mechanisms remain controversial.

Utilizing the Hoxb5 reporter system to prospectively isolate long-term HSCs (LT-HSCs) and short-term HSCs (ST-HSCs), we found that young and aged LT-HSCs co-transplanted into the same recipients demonstrated nearly equivalent myeloid lineage output, contrary to the theory of myeloid-biased HSC clones. Transcriptomics indicated no significant myeloid gene enrichment in aged LT-HSCs compared to their young counterparts. Instead, transplanting reconstituted young HSCs with the ratio of LT/ST-HSCs seen in aged mice can significantly skew the lineage output to myeloid cells. In addition, while the niche environment in the bone marrow minimally affects myeloid-biased hematopoiesis, aged thymi and spleens substantially hinder lymphoid hematopoiesis, resulting in further myeloid-domination. Thus, we demonstrate that myeloid-biased hematopoiesis in aged organisms originates due to alteration of the ratio between LT-HSCs and ST-HSCs rather than in heterogeneous HSC clones with various cell fates.

Introduction

Age-associated changes in individuals are deeply correlated with progressive attenuation of cellular functions in tissue stem cells of organs (Jones and Rando 2011). In the hematopoietic system, hematopoietic stem cells (HSCs), which possess self-renewal capacity and multipotency (Spangrude et al., 1988; Weissman and Shizuru 2008; Majeti et al., 2007), are responsible for various hematopoietic alterations with age, such as reduced self-renewal capacity (Morrison et al., 1996) and myeloid-biased hematopoiesis (Muller-Sieburg et al., 2004; Challen et al., 2010) due to their functional decline. For example, myeloid-biased hematopoiesis potentially reduces response to infections (Webster, 2000), reduces vaccination efficacy (Crooke et al., 2019), and increases myeloid malignancy (Rossi et al., 2008) in aged individuals. To comprehend these age-associated physiological changes, myeloid-biased hematopoiesis has been studied in considerable detail.

Based on the experimental observation that transplantation of aged HSCs exhibits more myeloid-biased differentiation in young recipient mice than transplantation of young HSCs, this phenotype has been thought to originate in cell-intrinsic changes in the HSC compartment (Geiger et al., 2013; De Haan and Lazare 2018; Schultz and Sinclair 2016). A myeloid-biased phenotype after aged HSC transplantation leads to the suggestion that myeloid-biased HSC clones selectively expand with age (Cho et al., 2008; Pang et al., 2011). Transcriptome and epigenetic analyses showing that a set of genes related to myeloid differentiation is significantly enriched in aged HSCs compared to young HSCs (Rossi et al., 2005; Grover et al., 2016) further supports this hypothesis.

On the other hand, some reports support a different point of view in light of experimental evidence showing that aged lymphoid-biased HSCs still demonstrate the same level of

89 lymphopoiesis as their younger counterparts, despite exhibiting a myeloid-biased gene
90 expression pattern (Montecino-Rodriguez et al., 2019). This result highlights the
91 limitations of predicting a pattern of HSC differentiation based upon gene expression
92 patterns. Moreover, myeloid progenitors such as granulocyte-macrophage progenitor
93 (GMP) and common myeloid progenitor (CMP) should also increase with age if the
94 selective expansion of myeloid-biased HSCs leads to an increase of myeloid cells in
95 peripheral blood (PB). However, increment of such progenitors with age was not
96 consistently demonstrated in earlier research (Rossi et al., 2005; Nilsson et al., 2016; Min
97 et al., 2006). Additionally, a mathematical model demonstrated that aging had no effect
98 on the daily production of CMP supplied from multipotent progenitors (MPP) (Busch et
99 al., 2015; Dorshkind et al., 2020).
100 As such, while selective expansion of myeloid-biased HSC clones is the most widely
101 accepted hypothesis to explain myeloid-biased hematopoiesis in aging (Mejia-Ramirez
102 and Florian, 2020; SanMiguel et al., 2020), other mechanisms may exist in light of the
103 inconsistent cellular behavior of progenitor fractions relative to HSCs. To the best of our
104 knowledge, no reports have analyzed kinetics of age-associated changes in HSCs,
105 progenitors, and PB cells simultaneously. Therefore, we started our investigation by
106 examining the correlation between age-related changes in PB and BM to shed light on
107 the mechanism underlying myeloid-biased hematopoiesis that occurs during aging.
108
109 **Results**
110 ***The discrepancy of age-associated alternation in peripheral blood and bone marrow***
111 ***calls into question the existence of a myeloid-biased clone***

112 Mouse HSC research on aging has used mice aged 18 months or older (Challen et al.,
113 2010; Cho et al., 2008; D. J. Rossi et al., 2005; Grover et al., 2016; Montecino-Rodriguez
114 et al., 2019; Nilsson et al., 2016). However, given that continuous accumulation of
115 cellular stress with age causes a gradual decline of cellular functions, a comprehensive
116 analysis from young to old mice is necessary to unravel mechanisms by which age-
117 associated, myeloid-biased hematopoiesis progress. Hence, we analyzed changes in PB
118 (**Fig. S1 A**) at multiple time points from young to old mice. These results showed that the
119 percentage of myeloid cells began to change as early as 6 months in mice and continued
120 to increase at a constant rate until the age of ≥ 23 months (**Fig. 1 A**).

121 It has been reported that myeloid-biased hematopoiesis is caused by a selective increase
122 of myeloid-biased clones in the immunophenotypically defined (surface-antigen
123 defined) HSC fraction (**Fig. S1 B**) (Beerman et al., 2010). According to this hypothesis,
124 age-associated myeloid hematopoiesis progression in PB would be paralleled by an
125 increase in myeloid-biased HSC clones. Therefore, we examined the frequency of the
126 HSC and progenitor fractions in the BM at multiple time points (**Fig. S1, B and C**). We
127 found that the frequency of immunophenotypically defined HSC in BM rapidly increased
128 up to the age of 12 months. After the age, the rate of increase in their frequency appeared
129 to slow down. (**Fig. 1 B**). On the other hand, in contrast to what we anticipated, the
130 frequency of GMP was stable, and the percentage of CMP actually decreased
131 significantly with age, defying our prediction that the frequency of components of the
132 myeloid differentiation pathway, such as CMP, GMP, and MEP would increase in aged
133 mice if myeloid-biased HSC clones increase with age (**Fig. 1 B**).

134 Finally, we determined the ratio of each fraction in young mice versus aged mice to
135 compare the age-associated transition pattern of components comprising the myeloid

136 differentiation pathway. Our analysis of hematopoietic alternations with age revealed that
137 age-associated transition patterns of immunophenotypically defined HSC and CMP in
138 BM were not paralleled with myeloid cell in PB (**Fig. 1 C**). These findings called into
139 question the hypothesis that there is a selective increase of myeloid-biased HSC clones
140 in the aged BM. We then set out to elucidate the mechanism by which myeloid-biased
141 phenotypes arise in the PB of aged mice.
142
143 ***The long-term observation of 2-year-old LT-HSC's differentiation does not indicate the***
144 ***expansion of myeloid-biased clones.***
145 Numerous studies have claimed that the myeloid-skewed phenotype observed in PB of
146 aged mice is caused by myeloid-biased HSC clones selectively expanded from HSCs with
147 originally heterogeneous differentiation potentials (Beerman et al., 2010; Dykstra et al.,
148 2011; Sudo et al., 2000). Other studies have reported that immunophenotypically defined
149 HSCs possess heterogeneity associated with self-renewal capacity, suggesting the
150 existence of at least two different populations in the HSC compartment, LT-HSCs and
151 ST-HSCs (Morrison and Weissman 1994; Spangrude et al., 1995). Since LT-HSCs have
152 extensive self-renewal capacity, while ST-HSCs lose their self-renewal capacity within a
153 short period, LT-HSCs are thought to persist in the BM throughout life and to enrich age-
154 associated changes compared to ST-HSCs. Therefore, we expect that LT-HSC-specific
155 analyses will help to answer whether myeloid-biased HSC clones exist.
156 We previously reported that Hoxb5 exclusively marks LT-HSCs in young mice (Chen et
157 al., 2016). However, we have not tested in aged mice whether Hoxb5 specifically labels
158 LT-HSCs and helps to distinguish LT-HSCs and ST-HSCs from immunophenotypically
159 defined HSCs (hereafter, bulk-HSCs). To confirm this, we first analyzed expression of

160 Hoxb5 in bulk-HSC, MPP, Flk2^{+}, and Lin^{-}Sca1^{-}c-Kit^{+} populations in aged *Hoxb5*-tri-
161 mCherry mice. We observed that Hoxb5 was exclusively expressed in bulk-HSCs (**Fig.**
162 **2 A**). Then, to verify long-term engraftment, we conducted a transplantation assay
163 utilizing Hoxb5^{+} HSCs and Hoxb5^{-} HSCs, respectively, isolated from 2-year-old mice
164 (**Fig. 2 B**). We observed that only recipients receiving aged Hoxb5^{+} HSCs exhibited
165 continuous hematopoiesis 16 weeks after primary transplantation (**Fig. 2, C and E; Fig.**
166 **S2 A**). In secondary transplantation analysis, only recipients receiving Hoxb5^{+} HSCs
167 exhibited robust hematopoiesis throughout the period of observation, indicating that
168 Hoxb5 can be used as a specific marker of LT-HSCs in aged mice, as well as young mice
169 (**Fig. 2, D and F; Fig. S2 B**).
170 A serial transplantation assay with a period of observation longer than 8 months should
171 be long enough to observe further myeloid-biased change. If bulk-HSCs isolated from
172 aged mice are already enriched by myeloid-biased HSC clones, we should see more
173 myeloid-biased phenotypes 16 weeks after primary and the secondary transplantation.
174 However, we found that kinetics of the proportion of myeloid cells in PB were similar
175 across the primary and the secondary transplantation (**Fig. 2 G**). These results suggest the
176 following two possibilities: either myeloid-biased HSCs do not expand in the LT-HSC
177 fraction, or the expansion of myeloid-biased clones in 2-year-old mice has already
178 peaked.
179
180 ***Direct comparison between young vs. aged LT-HSC differentiation reveals that LT-***
181 ***HSCs exhibit unchanged lineage output throughout life***
182 We developed a co-transplantation assay to directly compare the differentiation capacity
183 between young and aged LT-HSCs by co-transplanting ten young GFP^{+} LT-HSCs and

184 ten aged GFP$^-$ LT-HSCs into the same recipient mice (**Fig. 3 A**). Then, we found that the
185 myeloid lineage proportions from young and aged LT-HSCs were nearly comparable
186 during the observation period after transplantation (**Fig. 3, B and C**). Furthermore, by
187 analyzing the proportion of mature cell types derived from young and aged LT-HSCs in
188 the same donor, we directly compared the capacity for hematopoietic reconstitution in
189 each mature cell type between young and aged LT-HSCs. We confirmed again that the
190 reconstitution ratio was almost the same across all lineages, although bulk hematopoiesis
191 derived from young LT-HSCs predominated (**Fig. 3 D**). These results indicate that the
192 differentiation potential of LT-HSCs remains unchanged throughout their lives.
193 Several reports have demonstrated that transplanting mixed/bulk-HSCs—a combination
194 of LT-HSCs and ST-HSCs—obtained from old animals results in blatantly myeloid-
195 biased hematopoiesis (Beerman et al., 2010; Dykstra et al., 2011; Sudo et al., 2000). To
196 test this, we co-transplanted bulk-HSCs from young and old mice to corroborate this (**Fig.
197 S3 A**). As previously described, we observed that aged bulk-HSC exhibited a myeloid-
198 skewed phenotype (**Fig. S3 B and C**). Additionally, we observed that aged bulk-HSC
199 reconstitution exhibited higher reconstitution of myeloid cells compared to young bulk-
200 HSCs (**Fig. S3 D**). These findings unmistakably demonstrated that mixed/bulk-HSCs
201 showed myeloid skewed hematopoiesis in PB with aging, while LT-HSCs exhibited
202 unchanged lineage output throughout life.
203
204 ***LT-HSCs never show myeloid-related gene set enrichment during aging***
205 Although the results of co-transplantation of young and aged LT-HSCs did not
206 demonstrate lineage-biased output by LT-HSCs throughout life, enrichment of myeloid
207 genes in aged bulk-HSCs shown by previous studies supports the idea that myeloid-

208 biased hematopoiesis is caused by selective expansion of myeloid-biased HSC clones (D.
209 J. Rossi et al., 2005; Grover et al., 2016). To compare age-associated myeloid gene
210 enrichment, we isolated bulk-HSC, LT-HSCs, and ST-HSCs from young or aged mice
211 (**Fig. 4 A**).
212 To ensure the quality of the sorted fraction for subsequent RNA-seq analyses, we verified
213 the Hoxb5 read counts (**Fig. S4 A**). Cluster dendrograms using the whole transcriptome
214 confirmed that cell fractions isolated from young and aged mice clustered into distinct
215 groups (**Fig. 4 B**). Then, using sets of aging-related genes, such as inflammation
216 (Liberzon et al., 2015; Pietras 2017), DNA damage (p53 pathway) (Liberzon et al., 2015;
217 D. J. Rossi et al., 2007), cell cycle progression (E2F target) (Liberzon et al., 2015;
218 Kowalczyk et al., 2015), and a common aging signature (Flohr Svendsen et al., 2021), we
219 ran a violin plot analysis on each cell fraction to confirm the occurrence of typical aging-
220 related gene expression changes. We found age-associated changes in inflammation and
221 the DNA damage between cells isolated from young and aged mice, but very similar
222 patterns regardless of cell fraction in young or aged mice. In terms of cell cycle
223 progression and aging signature genes, however, we discovered that only the young LT-
224 HSC fraction differed from other young fractions and tended to represent similar gene
225 expression pattern with aged fractions (**Fig. 4 C**). Then, taking LT-HSC specific gene
226 expression pattern into account, we looked at expression patterns of specific genes that
227 had been highly validated by experiments as being associated with myeloid-biased HSC
228 (Beerman et al., 2010; Flohr Svendsen et al., 2021; Sanjuan-Pla et al., 2013; Mann et al.,
229 2018). We discovered that expression of these genes is relatively comparable between
230 young and aged LT-HSCs, but not other fractions (**Fig. S4 B**).

231 A recent comprehensive analysis of mouse HSC aging using multiple RNAseq data sets
232 claimed that almost 80% of differentially expressed genes are poorly reproducible across
233 data sets (Flohr Svendsen et al., 2021). In fact, we found that almost 80% of genes are
234 not shared when we compare three representative myeloid/lymphoid gene sets (Sanjuan-
235 Pla et al., 2013; Chambers et al., 2007; Pronk et al., 2007). Additionally, most genes were
236 only used in a single gene set (**Fig. 4, D and E**). By using only genes that were shared in
237 these gene sets, we ran a gene set enrichment analysis (GSEA) to see whether
238 myeloid/lymphoid genes were enriched in aged LT-HSCs or other fractions. Neither aged
239 LT-HSCs nor aged ST-HSCs exhibited myeloid/lymphoid gene set enrichment, while
240 shared myeloid-related genes tended to be enriched in aged bulk-HSCs, although this
241 enrichment was not statistically significant (**Fig. 4, F and G**). On the other hand, GSEA
242 analysis using original gene sets, respectively, showed inconsistent results (**Fig. S4, C**
243 **and D**).
244
245 ***A myeloid-biased phenotype in peripheral blood depends on the relative decrease of***
246 ***ST-HSC in the HSC compartment with age***
247 While transplantation of aged bulk-HSCs exhibits a myeloid-biased phenotype in PB
248 shown in previous reports (Beerman et al., 2010; Dykstra et al., 2011; Sudo et al., 2000)
249 and our results (**Fig. S3**), aged LT-HSCs remain stable in terms of the balance of their
250 differentiation potential between myeloid and lymphoid production (**Fig. 3**). Comparative
251 transcriptome analyses demonstrated that neither LT-HSCs nor ST-HSCs, which are
252 functionally more homogeneous than bulk-HSCs, exhibited myeloid gene set enrichment
253 with age, whereas aged bulk-HSCs tended to show more myeloid gene set enrichment

254 than their young counterparts (**Fig. 4**). We then tried to figure out what causes the
255 myeloid-biased phenotype in PB after transplantation of bulk-HSCs.
256 Because LT-HSCs in bulk-HSCs exhibit nearly constant level of hematopoiesis
257 throughout life, we hypothesized that ST-HSCs could be the key to discovering
258 mechanisms underlying the myeloid-skewing phenomenon. First, we revisited our
259 previous study (Chen et al., 2016), which demonstrated that transplanted ST-HSCs
260 maintain lymphocyte production while rapidly losing myeloid lineage production in
261 recipients. This result may potentially indicate the presence of HSC clones with a
262 preference for lymphoid differentiation. Given that donor cells obtained from primary
263 recipients receiving ST-HSCs do not undergo hematopoiesis in secondary transplantation
264 (Chen et al., 2016), it is likely that all ST-HSCs have already lost their ability to self-
265 renew and have disappeared from the HSC fraction in primary recipients. To confirm this,
266 we transplanted ten LT-HSCs or ST-HSCs and then analyzed PB and BM (**Fig. 5 A**). As
267 we previously reported (Chen et al., 2016), donor-derived hematopoiesis eventually
268 becomes lymphocyte-dominant in PB of ST-HSC recipients over time (**Fig. 5 B**).
269 Subsequently, it was determined that the vast majority of T cell subsets are memory cells
270 (**Fig. 5, C and D**). In addition, unlike recipients receiving LT-HSCs, recipients receiving
271 ST-HSCs lacked any bulk-HSCs in their BM (**Fig. 5, E and F**). These results strongly
272 suggest that lymphoid-biased hematopoiesis observed after transplantation of ST-HSCs
273 is due to persistence of memory-type lymphocytes in PB, rather than to *de novo*
274 lymphopoiesis from lymphoid-biased HSC clones. Persistence of memory-type
275 lymphocytes from ST-HSCs may have led us to misinterpret mechanisms underlying
276 myeloid-biased hematopoiesis after aged bulk-HSC transplantation. To verify this

277 hypothesis, we examined kinetics of the LT-HSC/ST-HSC ratio in the bulk-HSC
278 population, revealing the ratio of ST-HSC to LT-HSC decreased with age (**Figure S5**).
279 Thus, we hypothesized that the relative decrease in the ST-HSC ratio in the aged bulk-
280 HSC fraction would lead to reduction of memory-type lymphocytes and myeloid-biased
281 hematopoiesis following transplantation of aged bulk-HSCs. To test this hypothesis, we
282 isolated LT-HSCs and ST-HSCs from young donor mice and reconstituted them with a
283 2:8 ratio (as in young mice) or a 5:5 ratio (as in aged mice) prior to transplanting them
284 (**Fig. 6 A**). Four weeks after transplantation, PB analysis revealed that both groups had
285 comparable patterns of hematopoiesis. In contrast, recipient mice transplanted with a 5:5
286 ratio began to exhibit more myeloid-biased hematopoiesis eight weeks after
287 transplantation, and by week 16, they produced significantly more myeloid cells than the
288 other group (**Fig. 6, B-D**). Additionally, we conducted further investigations to determine
289 whether lymphoid hematopoiesis could be accelerated by alteration of LT-HSC/ST-HSC
290 ratios using cells from aged mice. To verify this, we isolated aged LT-HSCs and ST-
291 HSCs and reconstituted them with a 5:5 ratio or a 2:8 ratio prior to transplantation (**Fig.
292 S6 A**). Peripheral blood analysis revealed that lymphoid lineage output in the recipient
293 mice transplanted with a 2:8 ratio was significantly greater than those with a 5:5 ratio
294 (**Fig. S6 B-D**). Based on these findings, we concluded that myeloid-biased hematopoiesis
295 observed following transplantation of aged HSCs was caused by a relative decrease in
296 ST-HSC in the bulk-HSC compartment in aged mice rather than the selective expansion
297 of myeloid-biased HSC clones.
298
299 ***Age-associated extramedullary changes accelerate myeloid-biased hematopoiesis***

300 We found that the fluctuating LT-HSC/ST-HSC ratio in the bulk-HSC compartment
301 corresponded with the myeloid-biased hematopoiesis associated with aging. In contrast,
302 the degree of myeloid bias observed in mice older than 23 months without transplantation
303 (**Fig. 1 A**; 49.0 ± 23.4%) was significantly greater than in recipient mice receiving young
304 mixed HSCs with a 5:5 ratio 16 weeks after transplantation (**Fig. 6 D;** 30.8 ± 30.8%).
305 This difference indicated that other intrinsic or extrinsic factors might exist in mice older
306 than 23 months to promote myeloid-biased hematopoiesis. To investigate this further, we
307 transplanted ten GFP^+ young LT-HSCs into young or 2-year-old recipient mice and
308 examined their PB (**Fig. 7 A**). We limited the observation period to 12 weeks because
309 many aged recipient mice had died prior to that point (**Fig. 7 B**). PB analysis revealed
310 that aged recipient mice receiving young LT-HSCs produced significantly more myeloid
311 cells than young recipient mice (**Fig. 7, C-E**). These results suggested that recipient-
312 dependent extrinsic factors, rather than intrinsic factors of transplanted HSCs, had a
313 greater impact on hematopoietic cell differentiation. Then, we examined BM to determine
314 what extrinsic factors affected differentiation of transplanted HSCs. We performed BM
315 analysis for the mice denoted by † in Figure 7C because many of the aged mice had died
316 before the analysis. Percentages of CMP and GMP, downstream components of myeloid
317 differentiation, were stable or significantly lower in aged recipient mice than in young
318 recipient mice, just as they were in non-treated aged mice (**Fig. 7 F; Fig. 1 B**). In addition,
319 the percentage of CLP, a downstream component of lymphoid differentiation, did not
320 differ between young and aged recipients (**Fig. 7 F**). In contrast to previous studies (Pinho
321 et al., 2018; Ergen et al., 2012), these findings suggested that intramedullary age-
322 associated changes may not have a significant impact on LT-HSC differentiation.

323 Thymi and spleens of recipient mice were then examined, as these are the structures of
324 lymphoid maturation and production of lymphoid progenitors following migration from
325 BM and prior to their appearance in PB. The thymus and spleen analyses were also
326 performed on the mice denoted by † in Figure 7C. Donor cells were not microscopically
327 detectable in the majority of aged recipient mice (**Fig. 7, G and I**), and quantitative
328 analysis using a flow cytometer revealed that the frequency of donor cells in spleens and
329 thymi of aged recipients was significantly lower than in young recipients (**Fig. 7, H and**
330 **J**). These results indicate that the process of lymphoid lineage differentiation is impaired
331 in the spleens and thymi of aged mice compared to young mice, or that differentiating
332 cells in the bone marrow do not successfully migrate into these secondary lymphoid
333 organs. These factors contribute to the enhanced myeloid-biased hematopoiesis in
334 peripheral blood due to a decrease in de novo lymphocyte production.
335

336 **Discussion**

337 Age-related, myeloid-biased hematopoiesis has been suggested as a potential reason for
338 the decline in acquired immunity in the elderly (Geiger et al., 2013). This process has
339 been linked to an increase in myeloid-biased HSC clones in the bulk-HSC fraction
340 identified by surface antigens through aging. By isolating LT-HSCs and ST-HSCs,
341 respectively, we discovered that age-related changes in the ratio of ST-HSCs to LT-HSCs
342 in bulk-HSCs is responsible for myeloid-biased hematopoiesis.
343 When aged bulk-HSCs were transplanted into young mice, post-transplant hematopoiesis
344 in recipient mice was significantly biased toward myeloid in PB compared to
345 transplantation of young bulk-HSCs (Beerman et al., 2010; Dykstra et al., 2011; Sudo et
346 al., 2000). Historically, this myeloid-biased hematopoiesis derived from aged bulk-HSCs

347 has been considered as evidence supporting expansion of myeloid-biased HSC clones
348 with aging (Geiger et al., 2013; de Haan and Lazare 2018). Other studies suggest that
349 blockage of lymphoid hematopoiesis in aged mice results in myeloid-skewed
350 hematopoiesis through alternative mechanisms. However, this result should be
351 interpreted carefully, since Busulfan was used for myeloablative treatment in this study
352 (Montecino-Rodriguez et al., 2019). To clarify the cause for this disparity, we chose to
353 examine the LT-HSC fraction, which persists in the BM for long periods of time and is
354 enriched for aging-related alterations. We discovered that post-transplant hematopoiesis
355 of aged LT-HSCs did not vary from that of young LT-HSCs in terms of differentiation
356 capacity. Expression of myeloid-related genes was not significantly altered when LT-
357 HSCs from young and aged mice were compared. Therefore, we inferred that age-related
358 myeloid-biased hematopoiesis cannot be attributed to an increase in myeloid-biased
359 HSCs, at least among LT-HSCs. Given that bulk-HSCs consist of LT-HSCs and ST-
360 HSCs, and that LT-HSCs exhibit no change in differentiation potential with age, we
361 hypothesized that ST-HSCs may be responsible for the myeloid-skewing phenotype in
362 PB. Transcriptomic analysis revealed no enrichment of myeloid-related genes in the ST-
363 HSC fraction, ruling out the possibility of an increase in myeloid-biased HSCs in the ST-
364 HSC fraction. Alternatively, we observed a proportionate decrease in ST-HSCs in bulk-
365 HSCs accompanying an increase in LT-HSCs. We postulated that this relative decrease
366 in ST-HSC ratio is responsible for myeloid-biased hematopoiesis. When isolated LT-
367 HSCs and ST-HSCs from young mice were reconstituted to replicate an aged BM type in
368 terms of the LT-HSC/ST-HSC ratio, we discovered that PB was strongly skewed towards
369 myeloid cells after transplantation of reconstituted HSCs. In contrast, transplantation of

370 reconstituted HSCs with a young BM type resulted in a significantly lymphoid-skewed
371 PB profile.
372 On the other hand, it has been reported that myeloid-biased HSCs have a more persistent
373 capacity for self-renewal (Muller-Sieburg et al., 2004). In fact, in our prior investigation
374 comparing PB 16 weeks post-transplant, myeloid cell production in PB was greater when
375 LT-HSCs were transplanted, while ST-HSC transplantation resulted in a considerable
376 increase in lymphoid cell production (Chen et al., 2016). It is therefore possible that the
377 LT-HSCs and ST-HSCs we isolated utilizing the Hoxb5 reporter system are myeloid- and
378 lymphoid-biased HSCs, respectively. However, the myeloid-producing capacity of LT-
379 HSCs and ST-HSCs 4 weeks post-transplantation is equivalent (Chen et al., 2016). In
380 contrast, 16 weeks after transplantation, ST-HSC transplant recipients demonstrate
381 negligible myeloid development and a predominance of lymphocytes, unlike LT-HSC
382 transplant recipients (Chen et al., 2016). These characteristics show that early post-
383 transplant ST-HSCs lack the phenotypic of lymphoid-biased HSCs. When ST-HSC-
384 transplanted BM cells are employed as donors for secondary transplantation, no donor-
385 cell-derived hematopoiesis is detected in recipients (Chen et al., 2016). In addition, HSCs
386 are not observed in the BM following transplantation of ST-HSCs (**Fig. 5**). These results
387 indicate that ST-HSCs lose their capacity for self-renewal earlier after transplantation
388 than LT-HSCs. In addition, phenotypic examination of lymphocytes in PB after ST-HSC
389 transplantation revealed that nearly all of them were memory cells, and that there was no
390 *de novo* supply of T cells. In other words, ST-HSCs may have been erroneously classified
391 as lymphoid-biased HSCs due to the preservation of memory lymphocytes with a long
392 half-life in the peripheral circulation, despite the absence of *de novo* hematopoiesis
393 following transplantation of ST-HSCs. These findings suggest that the bias toward

394 myeloid and lymphoid lineages in post-transplant PB is not regulated by heterogeneity of
395 multipotency, but by heterogeneity of self-renewal capacity.
396 Multiple extrinsic factors have been implicated as HSC-independent causes of myeloid-
397 biased hematopoiesis associated with aging. Some findings suggest that cell interaction
398 with niche cells in BM is altered (Pinho et al., 2018), whereas others claim that chronic
399 inflammation in aged mice lowers production of lymphoid progenitors and induces
400 myeloid-biased hematopoiesis (Montecino-Rodriguez et al., 2019; Ergen et al., 2012). To
401 identify HSC-independent causes of myeloid-biased hematopoiesis specifically, we
402 transplanted young LT-HSCs into young or aged mice. Cellular differentiation observed
403 in BM revealed that proportions of GMP, MEP, and CLP are unchanged between young
404 and aged recipients. In contrast, an examination of spleens and thymi, the sites of
405 lymphocyte maturation, revealed the absence of donor cells in aged recipients. These
406 findings suggest that myeloid cells increase in aging mice due to a relative decrease in
407 the ratio of mature lymphocytes in PB, resulting from inhibition of lymphocyte
408 maturation outside the BM, such as in the thymus and spleen, rather than a significant
409 change in cell differentiation caused by the intramedullary environment. Attempts have
410 been made in the past to restore thymus function in aged mice by administering
411 keratinocyte growth factor (KGF) (S. W. Rossi et al., 2007). Indeed, in aged mice,
412 lymphocyte hematopoiesis recovers, which is consistent with our results that the
413 extramedullary environment influences the myeloid-bias phenotype in PB (S. W. Rossi
414 et al., 2007).
415 It has been clinically documented that recovery of the lymphocyte fraction in PB is
416 delayed in elderly donors, compared to young donors (González-Vicent et al., 2017;
417 Baron et al., 2006). Although it is undeniable that this phenomenon may be due to

418 decreased HSC hematopoietic potential, it may also be due to a change in the ratio of LT-
419 HSC/ST-HSCs in bulk-HSCs, as described in our report, which may give the appearance
420 of a myeloid bias in PB after transplantation. It has also been noted that lymphocyte
421 recovery is delayed in elderly patients compared to younger patients (Berger et al., 2008;
422 van der Maas et al., 2021). Age-related loss in thymus and spleen functions has been
423 recorded in humans, implying that the same mechanism is acting as in our mouse
424 observations. If it is possible to assess and regulate the LT-HSC/ST-HSC ratio in donors
425 and thymus/spleen function in recipients in the future, it will help to develop accurate
426 models for predicting lymphocyte recovery after transplantation as well as new
427 transplantation strategies.
428 In contrast, our findings should be considered in light of some limitations. In this report,
429 we primarily performed ten to twenty cell transplantation assays. Therefore, the current
430 theory should be revalidated using single-cell technology with lineage tracing system
431 (Yamamoto et al. 2018; Rodriguez-Fraticelli et al. 2020). This approach will investigate
432 changes in the self-renewal capacity of individual HSCs and their subsequent
433 differentiation into progenitor cells and peripheral blood cells. Additionally, in this report
434 we purified LT-HSCs by Hoxb5 reporter system. In contrast, various LT-HSC markers
435 have been previously reported. Therefore, it is ideal to validate our findings using other
436 LT-HSC makers.
437 In summary, we have demonstrated for the first time that the ratio of LT-HSC/ST-HSC
438 is important in age-related myeloid skewed hematopoiesis as an HSC-dependent factor
439 and that aging-related thymus and spleen dysfunction also contributes significantly as an
440 HSC-independent factor. Furthermore, here we propose a "self-renewal heterogeneity
441 model" as a new mechanism for hematopoietic heterogeneity, including myeloid-biased

442 hematopoiesis in aged mice (**Fig. 8**). In addition to this report, we have also shown that
443 cellular differentiation in the PB after transplantation can vary by changing
444 transplantation conditions, ultimately altering self-renewal ability (Sakamaki et al., 2021;
445 Nishi et al., 2022). This highlights the significance of deciphering molecular processes
446 that regulate the heterogeneity of HSC self-renewal capacity, which will help to provide
447 a better understanding of the hematopoietic system and the hematopoietic hierarchy in
448 the future.
449

450 **Methods**

451 **Mice**

452 Mice with an *Hoxb5*-tri-mCherry (C57BL/6J background), derived from our previous
453 work (Chen et al., 2016), were harvested for donor cells for transplantation, PB, and BM
454 analysis. CAG-EGFP mice (C57BL/6J background) were bred with *Hoxb5*-tri-mCherry
455 for transplantation experiments. 8-14-week-old C57BL/6-Ly5.1 mice (purchased from
456 Sankyo Labo Service) were used as recipients for transplantation assays. For aged
457 recipients, 2-year-old CD45.2 C57BL/6J mice were purchased from CLEA Japan.
458 Supporting BM cells were collected from 8-12-week-old C57BL/6-Ly5.1 × C57BL/6J
459 (F_1 mice CD45.1$^+$/CD45.2$^+$). All mice were housed in specific pathogen-free (SPF)
460 conditions and were carefully observed by staff members. Mice were bred according to
461 RIKEN or Kyoto University. All animal protocols were approved by the RIKEN Center
462 for Biosystems Dynamics Research and Kyoto University.
463

464 **Flow cytometry, cell sorting, and bone marrow analyses**

465 Flow cytometry and cell sorting were performed on a FACS Aria II cell sorter (BD
466 Biosciences) and analyzed using FlowJo™ software (BD Biosciences). Bone marrow
467 (BM) cells were collected from bilateral tibias, femurs, humeri, and pelvises in Ca^{2+}- and
468 Mg^{2+}-free PBS supplemented with 2% heat-inactivated bovine serum (Gibco) and 2 mM
469 EDTA (Thermo Fisher Scientific). Cells were passed through 100-µm, and 40-µm
470 strainers (Corning) before analysis and sorting. Prior to staining, samples were blocked
471 with 50 ug/mL rat IgG (Sigma-Aldrich) for 15 min. To enrich HSCs and progenitor
472 populations for sorting and bone marrow analyses, cells were stained with APC-
473 eFluor780-conjugated anti-c-Kit (clone: 2B8) and fractionated using anti-APC magnetic
474 beads and LS columns (both Miltenyi Biotec). c-Kit^{+} cells were then stained with
475 combinations of antibodies as described in Supplemental Table 1. All staining was
476 incubated at 4°C for 30 min, except for CD34 staining, which was incubated for 90 min.
477 Samples were washed twice after staining. Prior to flow cytometry or cell sorting, samples
478 were stained with SYTOX Red Dead Cell Stain (Life Technologies) or 7-
479 aminoactinomycin D (BioLegend). Cells were double sorted for purity. For the combined
480 analysis of the upstream (HSC, MPP, Flk2+) and downstream (CLP, MEP, CMP, GMP)
481 fractions in Figures 1B and 7F, we normalized by c-Kit+ cells because we performed a
482 c-Kit enrichment for the bone marrow analysis.
483

484 **Transplantation and peripheral blood analyses**

485 12-24 hours prior to transplantation, C57BL/6-Ly5.1 mice, or aged C57BL/6J recipient
486 mice were lethally irradiated with single doses of 8.7 Gy or 9.1Gy. For transplantation
487 assays, donor cells were first combined with 2×10^5 whole bone marrow supporting cells
488 (C57BL/6-Ly5.1 × C57BL/6J F_1 mice CD45.1^{+}/CD45.2^{+}) in 200 µL of PBS with 2%

489 FBS, and then injected into the retro-orbital venous plexus. For evaluation of post-
490 transplant kinetics, PB was collected and analyzed. At each time point, 50 μL of blood
491 were collected from the tail vein and re-suspended in Ca^{2+}- and Mg^{2+}-free PBS
492 supplemented with 2 mM EDTA. Red blood cells were lysed twice on ice for 3 min with
493 BD Pharm Lyse Buffer (BD Pharmingen). Identification of leukocyte subsets was
494 performed by staining with antibodies. Antibody information was described in
495 Supplemental Table 1. For evaluation of lineage output, the frequency of each lineage
496 (NK cell, B cell, T cell, neutrophil, and monocyte) was determined in the whole fraction.
497 The analysis of donor lineage output was restricted to donor cells showing ≥ 0.1% donor
498 chimerism at the last PB analysis to allow reliable detection. The percentage of donor
499 chimerism in PB was defined as the percentage of $CD45.1^{-}CD45.2^{+}$ cells among total
500 $CD45.1^{-}CD45.2^{+}$ and $CD45.1^{+}CD45.2^{+}$ cells. PB data represents mice which survived
501 until the last PB analysis.
502
503 **Thymus and Spleen analysis**
504 Thymi and spleens were harvested and disrupted into a single cell suspension. Cells were
505 passed through 100-μm, and 40-μm strainers (Corning). Isolated thymocytes and
506 splenocytes were incubated on ice for 30 min with appropriately diluted antibodies in
507 staining buffer. Identification of B cells in spleens and T cells in thymi was performed
508 by staining with antibodies described in Supplemental Table 1. Prior to flow cytometry
509 or cell sorting, samples were stained with SYTOX Red Dead Cell Stain (Life
510 Technologies).
511
512 **Tissue imaging**

513 Freshly dissected spleens and thymi were fixed in 4% PFA (Nacalai tesque) in PBS for
514 24 h at 4°C. After PFA washout with PBS, tissues were cryoprotected with 30% sucrose
515 in PBS for 24 h at 4°C, embedded in Tissue-Tek O.C.T. compound (Sakura Finetek), and
516 snap-frozen in liquid nitrogen. Serial 10-μm longitudinal cryostat sections were obtained
517 using CryoStar NX50 (Thermo Fisher Scientific). Cell nuclei were counterstained with
518 4',6-diamidino-2-phenylindole (DAPI, 1 μg/mL, Roche). To reduce autofluorescence,
519 tissue sections were treated with Vector TrueVIEW autofluorescence quenching kit
520 (Vector Laboratories). Images were obtained from Leica TCS SP8 (Leica).
521

522 **RNA sequencing**

523 Total RNA was isolated with Trizol (Thermo Fisher Scientific) and cleaned up using
524 RNeasy MinElute columns (QIAGEN). cDNA libraries were prepared from bulk-HSCs,
525 ST-HSCs and LT-HSCs using a KAPA RNA HyperPrep kit with RiboErase (HMR)
526 (Kapa Biosystems) and sequenced using a Hiseq 1500 (Illumina) to obtain 2 × 127 base-
527 pair (bp) paired-end reads. Three replicates were sequenced for each population. Raw
528 transcriptome sequence data were mapped to the genome (mm10) using HISAT2 (ver
529 2.1.0) (Kim et al., 2015). Alignments were then passed to StringTie (ver 1.3.4d), which
530 was used to assemble and quantify transcripts in each sample (Pertea et al., 2016). EdgeR
531 (ver 3.22.5) was then used to compare all transcripts across conditions and to produce
532 tables and plots of differentially expressed genes and transcripts (Robinson et al., 2009).
533 Normalization with the TMM method was performed with the edgeR package in
534 Bioconductor (https://bioconductor.org/). Genes (12,808 genes) were selected for
535 hierarchical clustering based on the mean of TMM normalized read counts across all
536 samples' cells (mean ≥ 1). Then, clustering was performed by using the hclust function

537 for R (distance = Spearman's correlation'; method = 'ward.D2'). We depicted Venn
538 diagrams and performed GSEA analyses in Figures 4D-G and S4C-D using previously
539 published gene sets after excluding genes that could not be annotated by our
540 transcriptome dataset. GSEA was performed using GSEA software
541 (http://www.broadinstitute.org/gsea) with default settings (Subramanian et al., 2005).
542

543 **Quantification and statistical analyses**

544 Statistical analyses were performed using ggplot2 in R (version 4.1.2) or Microsoft Excel.
545 Sample size for each experiment and replicate numbers of experiments are included in
546 figure legends. Statistical significance was determined using Welch's t test. P values <
547 0.05 were considered significant.
548

549 **Data and materials availability**

550 Sequencing data has been deposited in the Gene Expression Omnibus under accession
551 code GSE226803. Correspondence and requests for materials should be addressed to
552 M.M. (miya75@med.kobe-u.ac.jp).
553

554 **Acknowledgements**

555 We gratefully acknowledge Hiroshi Kiyonari for animal care and providing recipient
556 mice at RIKEN BDR. Shigehiro Kuraku, Mitsutaka Kadota, and Chiharu Tanegashima
557 provided technical support for RNA sequencing and analysis at RIKEN BDR. Momo
558 Fujii performed imaging experiments at RIKEN BDR. Hitomi Oga, Kayoko Nagasaka,
559 and Masaki Miyahashi provided laboratory management at Kobe University. The authors
560 gratefully acknowledge ongoing support for this work: Masanori Miyanishi was

supported by the Japan Society for the Promotion of Science (JSPS) KAKENHI Grant Number JP17K07407 and JP20H03268, The Mochida Memorial Foundation for Medical and Pharmaceutical Research, The Life Science Foundation of Japan, The Takeda Science Foundation, The Astellas Foundation for Research on Metabolic Disorders, AMED-PRIME, AMED under Grant Number JP18gm6110020. Taro Sakamaki was supported by the JSPS Core-to-Core Program, JSPS KAKENHI Grant Numbers JP21K20669, JP22K16334, RIKEN Junior Research Associate Program. Katsuyuki Nishi was supported by JSPS Grant Numbers KAKENHI JP18J13408 and 23K15326.

Authorship Contributions

K.N. conceived, performed, analyzed the experiments. T.S. and K.S. performed transplantation experiments. M.M. conceived, performed, analyzed, and oversaw the experiments. K.N. and M.M. wrote the manuscript. T.S., A.N., K.S.K., K.S., M.A., N.Y., and A.T. provided comments on the manuscript.

Disclosure of Conflicts of Interest

The authors declare no conflicts of interest in relation to the present study.

References

Baron, Frédéric, Barry Storer, Michael B. Maris, Jan Storek, Fanny Piette, Monja Metcalf, Kristen White, et al. 2006. "Unrelated Donor Status and High Donor Age Independently Affect Immunologic Recovery after Nonmyeloablative Conditioning." *Biology of Blood and Marrow Transplantation* 12 (11): 1176–87. https://doi.org/10.1016/j.bbmt.2006.07.004.

Beerman, Isabel, Deepta Bhattacharya, Sasan Zandi, Mikael Sigvardsson, Irving L. Weissman, David Brydere, and Derrick J. Rossia. 2010. "Functionally Distinct Hematopoietic Stem Cells Modulate Hematopoietic Lineage Potential during Aging by a Mechanism of Clonal Expansion." *Proceedings of the National*

589 *Academy of Sciences of the United States of America* 107 (12): 5465–70.
590 https://doi.org/10.1073/pnas.1000834107.
591 Berger, Massimo, O. Figari, B. Bruno, A. Raiola, A. Dominietto, M. Fiorone, M.
592 Podesta, et al. 2008. "Lymphocyte Subsets Recovery Following Allogeneic Bone
593 Marrow Transplantation (BMT): CD4+ Cell Count and Transplant-Related
594 Mortality." *Bone Marrow Transplantation* 41 (1): 55–62.
595 https://doi.org/10.1038/sj.bmt.1705870.
596 Busch, Katrin, Kay Klapproth, Melania Barile, Michael Flossdorf, Tim Holland-Letz,
597 Susan M. Schlenner, Michael Reth, Thomas Höfer, and Hans Reimer Rodewald.
598 2015. "Fundamental Properties of Unperturbed Haematopoiesis from Stem Cells in
599 Vivo." *Nature* 518 (7540): 542–46. https://doi.org/10.1038/nature14242.
600 Challen, Grant A., Nathan C. Boles, Stuart M. Chambers, and Margaret A. Goodell.
601 2010. "Distinct Hematopoietic Stem Cell Subtypes Are Differentially Regulated by
602 TGF-B1." *Cell Stem Cell* 6 (3): 265–78.
603 https://doi.org/10.1016/j.stem.2010.02.002.
604 Chambers, Stuart M., Nathan C. Boles, Kuan Yin K. Lin, Megan P. Tierney, Teresa V.
605 Bowman, Steven B. Bradfute, Alice J. Chen, et al. 2007. "Hematopoietic
606 Fingerprints: An Expression Database of Stem Cells and Their Progeny." *Cell*
607 *Stem Cell* 1 (5): 578–91. https://doi.org/10.1016/j.stem.2007.10.003.
608 Chen, James Y., Masanori Miyanishi, Sean K. Wang, Satoshi Yamazaki, Rahul Sinha,
609 Kevin S. Kao, Jun Seita, Debashis Sahoo, Hiromitsu Nakauchi, and Irving L.
610 Weissman. 2016. "Hoxb5 Marks Long-Term Haematopoietic Stem Cells and
611 Reveals a Homogenous Perivascular Niche." *Nature* 530 (7589): 223–27.
612 https://doi.org/10.1038/nature16943.
613 Cho, Rebecca H., Hans B. Sieburg, and Christa E. Muller-Sieburg. 2008. "A New
614 Mechanism for the Aging of Hematopoietic Stem Cells: Aging Changes the Clonal
615 Composition of the Stem Cell Compartment but Not Individual Stem Cells." *Blood*
616 111 (12): 5553–61. https://doi.org/10.1182/blood-2007-11-123547.
617 Crooke, Stephen N., Inna G. Ovsyannikova, Gregory A. Poland, and Richard B.
618 Kennedy. 2019. "Immunosenescence and Human Vaccine Immune Responses."
619 *Immunity & Ageing* 16 (1): 1–16. https://doi.org/10.1186/s12979-019-0164-9.
620 Dorshkind, Kenneth, Thomas Höfer, Encarnacion Montecino-Rodriguez, Peter D. Pioli,
621 and Hans Reimer Rodewald. 2020. "Do Haematopoietic Stem Cells Age?" *Nature*
622 *Reviews Immunology* 20 (3): 196–202. https://doi.org/10.1038/s41577-019-0236-2.
623 Dykstra, Brad, Sandra Olthof, Jaring Schreuder, Martha Ritsema, and Gerald de Haan.
624 2011. "Clonal Analysis Reveals Multiple Functional Defects of Aged Murine
625 Hematopoietic Stem Cells." *The Journal of Experimental Medicine* 208 (13):
626 2691–2703. https://doi.org/10.1084/jem.20111490.
627 Dykstra, Brad, Sandra Olthof, Jaring Schreuder, Martha Ritsema, and Gerald De Haan.
628 2011. "Clonal Analysis Reveals Multiple Functional Defects of Aged Murine
629 Hematopoietic Stem Cells." *Journal of Experimental Medicine* 208 (13): 2691–
630 2703. https://doi.org/10.1084/jem.20111490.
631 Ergen, Aysegul V., Nathan C. Boles, and Margaret A. Goodell. 2012. "Rantes/Ccl5
632 Influences Hematopoietic Stem Cell Subtypes and Causes Myeloid Skewing."
633 *Blood* 119 (11): 2500–2509. https://doi.org/10.1182/blood-2011-11-391730.
634 Flohr Svendsen, Arthur, Daozheng Yang, Kyung Mok Kim, Seka Lazare, Natalia
635 Skinder, Erik Zwart, Anna Mura-Meszaros, et al. 2021. "A Comprehensive

Transcriptome Signature of Murine Hematopoietic Stem Cell Aging." *Blood* 138 (6): 439–51. https://doi.org/10.1182/blood.2020009729.

Geiger, Hartmut, Gerald De Haan, and M. Carolina Florian. 2013. "The Ageing Haematopoietic Stem Cell Compartment." *Nature Reviews Immunology* 13 (5): 376–89. https://doi.org/10.1038/nri3433.

González-Vicent, Marta, Blanca Molina, Natalia Deltoro, Julián Sevilla, José Luis Vicario, Ana Castillo, Manuel Ramirez, and Miguel Ángel Díaz. 2017. "Donor Age Matters in T-Cell Depleted Haploidentical Hematopoietic Stem Cell Transplantation in Pediatric Patients: Faster Immune Reconstitution Using Younger Donors." *Leukemia Research* 57: 60–64. https://doi.org/10.1016/j.leukres.2017.03.001.

Grover, Amit, Alejandra Sanjuan-Pla, Supat Thongjuea, Joana Carrelha, Alice Giustacchini, Adriana Gambardella, Iain Macaulay, et al. 2016. "Single-Cell RNA Sequencing Reveals Molecular and Functional Platelet Bias of Aged Haematopoietic Stem Cells." *Nature Communications* 7. https://doi.org/10.1038/ncomms11075.

Haan, Gerald de, and Seka Simone Lazare. 2018. "Aging of Hematopoietic Stem Cells." *Blood* 131 (5): 479–87. https://doi.org/10.1182/blood-2017-06-746412.

Haan, Gerald De, and Seka Simone Lazare. 2018. "Aging of Hematopoietic Stem Cells." www.bloodjournal.org.

Jones, D. Leanne, and Thomas A. Rando. 2011. "Emerging Models and Paradigms for Stem Cell Ageing." *Nature Cell Biology* 13 (5): 506–12. https://doi.org/10.1038/ncb0511-506.

Kim, Daehwan, Ben Langmead, and Steven L. Salzberg. 2015. "HISAT: A Fast Spliced Aligner with Low Memory Requirements." *Nature Methods* 12 (4): 357–60. https://doi.org/10.1038/nmeth.3317.

Kowalczyk, Monika S., Itay Tirosh, Dirk Heckl, Tata Nageswara Rao, Atray Dixit, Brian J. Haas, Rebekka K. Schneider, Amy J. Wagers, Benjamin L. Ebert, and Aviv Regev. 2015. "Single-Cell RNA-Seq Reveals Changes in Cell Cycle and Differentiation Programs upon Aging of Hematopoietic Stem Cells." *Genome Research* 25 (12): 1860–72. https://doi.org/10.1101/gr.192237.115.

Liberzon, Arthur, Chet Birger, Helga Thorvaldsdóttir, Mahmoud Ghandi, Jill P. Mesirov, and Pablo Tamayo. 2015. "The Molecular Signatures Database Hallmark Gene Set Collection." *Cell Systems* 1 (6): 417–25. https://doi.org/10.1016/j.cels.2015.12.004.

Maas, Nicolaas G. van der, Erik G.J. von Asmuth, Dagmar Berghuis, Pauline A. van Schouwenburg, Hein Putter, Mirjam van der Burg, and Arjan C. Lankester. 2021. "Modeling Influencing Factors in B-Cell Reconstitution After Hematopoietic Stem Cell Transplantation in Children." *Frontiers in Immunology* 12 (May): 1–8. https://doi.org/10.3389/fimmu.2021.684147.

Majeti, Ravindra, Christopher Y. Park, and Irving L. Weissman. 2007. "Identification of a Hierarchy of Multipotent Hematopoietic Progenitors in Human Cord Blood." *Cell Stem Cell* 1 (6): 635–45. https://doi.org/10.1016/j.stem.2007.10.001.

Mann, Mati, Arnav Mehta, Carl G de Boer, Monika S Kowalczyk, Kevin Lee, Pearce Haldeman, Noga Rogel, et al. 2018. "Heterogeneous Responses of Hematopoietic Stem Cells to Inflammatory Stimuli Are Altered with Age." *Cell Reports* 25 (11): 2992–3005. https://doi.org/10.1016/j.celrep.2018.11.056.

683 Mejia-Ramirez, Eva, and Maria Carolina Florian. 2020. "Understanding Intrinsic
684 Hematopoietic Stem Cell Aging." *Haematologica* 105 (1): 22–37.
685 https://doi.org/10.3324/haematol.2018.211342.
686 Min, Hyeyoung, Encarnacion Montecino-Rodriguez, and Kenneth Dorshkind. 2006.
687 "Effects of Aging on the Common Lymphoid Progenitor to Pro-B Cell Transition."
688 *The Journal of Immunology* 176 (2): 1007–12.
689 https://doi.org/10.4049/jimmunol.176.2.1007.
690 Montecino-Rodriguez, Encarnacion, Ying Kong, David Casero, Adrien Rouault,
691 Kenneth Dorshkind, and Peter D. Pioli. 2019. "Lymphoid-Biased Hematopoietic
692 Stem Cells Are Maintained with Age and Efficiently Generate Lymphoid
693 Progeny." *Stem Cell Reports* 12 (3): 584–96.
694 https://doi.org/10.1016/j.stemcr.2019.01.016.
695 Morrison, Sean J., and Irving L. Weissman. 1994. "The Long-Term Repopulating
696 Subset of Hematopoietic Stem Cells Is Deterministic and Isolatable by
697 Phenotype." *Immunity* 1 (8): 661–73. https://doi.org/10.1016/1074-
698 7613(94)90037-X.
699 Morrison, Sean J, A M Wandycz, K Akashi, A Globerson, and Irving L Weissman.
700 1996. "The Aging of Hematopoietic Stem Cells." *Nature Medicine* 2 (9): 1011–16.
701 https://doi.org/10.1038/nm0996-1011.
702 Muller-Sieburg, Christa E., Rebecca H. Cho, Lars Karlsson, Jing F. Huang, and Hans B.
703 Sieburg. 2004. "Myeloid-Biased Hematopoietic Stem Cells Have Extensive Self-
704 Renewal Capacity but Generate Diminished Lymphoid Progeny with Impaired IL-
705 7 Responsiveness." *Blood* 103 (11): 4111–18. https://doi.org/10.1182/blood-2003-
706 10-3448.
707 Nilsson, Alexandra Rundberg, Shamit Soneji, Sofia Adolfsson, David Bryder, and
708 Cornelis Jan Pronk. 2016. "Human and Murine Hematopoietic Stem Cell Aging Is
709 Associated with Functional Impairments and Intrinsic Megakaryocytic/Erythroid
710 Bias." *PLoS ONE* 11 (7): 1–20. https://doi.org/10.1371/journal.pone.0158369.
711 Nishi, Katsuyuki, Taro Sakamaki, Kay Sadaoka, Momo Fujii, Akifumi Takaori-Kondo,
712 James Y. Chen, and Masanori Miyanishi. 2022. "Identification of the Minimum
713 Requirements for Successful Haematopoietic Stem Cell Transplantation." *British*
714 *Journal of Haematology* 196 (3): 711–23. https://doi.org/10.1111/bjh.17867.
715 Pang, Wendy W., Elizabeth A. Price, Debashis Sahoo, Isabel Beerman, William J.
716 Maloney, Derrick J. Rossi, Stanley L. Schrier, and Irving L. Weissman. 2011.
717 "Human Bone Marrow Hematopoietic Stem Cells Are Increased in Frequency and
718 Myeloid-Biased with Age." *Proceedings of the National Academy of Sciences of*
719 *the United States of America* 108 (50): 20012–17.
720 https://doi.org/10.1073/pnas.1116110108.
721 Pertea, Mihaela, Daehwan Kim, Geo M. Pertea, Jeffrey T. Leek, and Steven L.
722 Salzberg. 2016. "Transcript-Level Expression Analysis of RNA-Seq Experiments
723 with HISAT, StringTie and Ballgown." *Nature Protocols* 11 (9): 1650–67.
724 https://doi.org/10.1038/nprot.2016.095.
725 Pietras, Eric M. 2017. "Inflammation: A Key Regulator of Hematopoietic Stem Cell
726 Fate in Health and Disease." *Blood* 130 (15): 1693–98.
727 https://doi.org/10.1182/blood-2017-06-780882.
728 Pinho, Sandra, Tony Marchand, Eva Yang, Qiaozhi Wei, Claus Nerlov, and Paul S.
729 Frenette. 2018. "Lineage-Biased Hematopoietic Stem Cells Are Regulated by

Distinct Niches." *Developmental Cell* 44 (5): 634-641.e4. https://doi.org/10.1016/j.devcel.2018.01.016.

Pronk, Cornelis J.H., Derrick J. Rossi, Robert Månsson, Joanne L. Attema, Gudmundur Logi Norddahl, Charles Kwok Fai Chan, Mikael Sigvardsson, Irving L. Weissman, and David Bryder. 2007. "Elucidation of the Phenotypic, Functional, and Molecular Topography of a Myeloerythroid Progenitor Cell Hierarchy." *Cell Stem Cell* 1 (4): 428–42. https://doi.org/10.1016/j.stem.2007.07.005.

Robinson, Mark D., Davis J. McCarthy, and Gordon K. Smyth. 2009. "EdgeR: A Bioconductor Package for Differential Expression Analysis of Digital Gene Expression Data." *Bioinformatics* 26 (1): 139–40. https://doi.org/10.1093/bioinformatics/btp616.

Rodriguez-Fraticelli, Alejo E., Caleb Weinreb, Shou Wen Wang, Rosa P. Migueles, Maja Jankovic, Marc Usart, Allon M. Klein, Sally Lowell, and Fernando D. Camargo. 2020. "Single-Cell Lineage Tracing Unveils a Role for TCF15 in Haematopoiesis." *Nature* 583 (7817): 585–89. https://doi.org/10.1038/s41586-020-2503-6.

Rossi, Derrick J., David Bryder, Jun Seita, Andre Nussenzweig, Jan Hoeijmakers, and Irving L. Weissman. 2007. "Deficiencies in DNA Damage Repair Limit the Function of Haematopoietic Stem Cells with Age." *Nature* 447 (7145): 725–29. https://doi.org/10.1038/nature05862.

Rossi, Derrick J., Catriona H.M. Jamieson, and Irving L. Weissman. 2008. "Stems Cells and the Pathways to Aging and Cancer." *Cell* 132 (4): 681–96. https://doi.org/10.1016/j.cell.2008.01.036.

Rossi, Derrick J, David Bryder, Jacob M Zahn, Henrik Ahlenius, Rebecca Sonu, Amy J Wagers, and Irving L Weissman. 2005. "Cell Intrinsic Alterations Underlie Hematopoietic Stem Cell Aging." *Proceedings of the National Academy of Sciences of the United States of America* 102 (26): 9194–99. https://doi.org/10.1073/pnas.0503280102.

Rossi, Simona W., Lukas T. Jeker, Tomoo Ueno, Sachiyo Kuse, Marcel P. Keller, Saulius Zuklys, Andrei V. Gudkov, et al. 2007. "Keratinocyte Growth Factor (KGF) Enhances Postnatal T-Cell Development via Enhancements in Proliferation and Function of Thymic Epithelial Cells." *Blood* 109 (9): 3803–11. https://doi.org/10.1182/blood-2006-10-049767.

Sakamaki, Taro, Kevin S. Kao, Katsuyuki Nishi, James Y. Chen, Kay Sadaoka, Momo Fujii, Akifumi Takaori-Kondo, Irving L. Weissman, and Masanori Miyanishi. 2021. "Hoxb5 Defines the Heterogeneity of Self-Renewal Capacity in the Hematopoietic Stem Cell Compartment." *Biochemical and Biophysical Research Communications* 539 (February): 34–41. https://doi.org/10.1016/j.bbrc.2020.12.077.

Sanjuan-Pla, Alejandra, Iain C. Macaulay, Christina T. Jensen, Petter S. Woll, Tiago C. Luis, Adam Mead, Susan Moore, et al. 2013. "Platelet-Biased Stem Cells Reside at the Apex of the Haematopoietic Stem-Cell Hierarchy." *Nature* 502 (7470): 232–36. https://doi.org/10.1038/nature12495.

SanMiguel, Jennifer M., Kira Young, and Jennifer J. Trowbridge. 2020. "Hand in Hand: Intrinsic and Extrinsic Drivers of Aging and Clonal Hematopoiesis." *Experimental Hematology* 91: 1–9. https://doi.org/10.1016/j.exphem.2020.09.197.

Schultz, Michael B., and David A. Sinclair. 2016. "When Stem Cells Grow Old: Phenotypes and Mechanisms of Stem Cell Aging." *Development (Cambridge)* 143 (1): 3–14. https://doi.org/10.1242/dev.130633.

Spangrude, Gerald J., Diane M. Brooks, and Daniel B. Tumas. 1995. "Long-Term Repopulation of Irradiated Mice with Limiting Numbers of Purified Hematopoietic Stem Cells: In Vivo Expansion of Stem Cell Phenotype but Not Function." *Blood* 85 (4): 1006–16. https://doi.org/10.1182/blood.v85.4.1006.bloodjournal8541006.

Spangrude, Gerald J, Shelly Heimfeld, and Irving L Weissman. 1988. "Purification and Characterization of Mouse Hematopoietic Stem Cells." *Science (New York, N.Y.)* 241 (4861): 58–62. https://doi.org/10.1126/science.2898810.

Subramanian, Aravind, Pablo Tamayo, Vamsi K. Mootha, Sayan Mukherjee, Benjamin L. Ebert, Michael A. Gillette, Amanda Paulovich, et al. 2005. "Gene Set Enrichment Analysis: A Knowledge-Based Approach for Interpreting Genome-Wide Expression Profiles." *Proceedings of the National Academy of Sciences of the United States of America* 102 (43): 15545–50. https://doi.org/10.1073/pnas.0506580102.

Sudo, K, H Ema, Y Morita, and H Nakauchi. 2000. "Age-Associated Characteristics of Murine Hematopoietic Stem Cells [In Process Citation]." *J Exp Med* 192 (9): 1273–80.

Webster, Robert G. 2000. "Immunity to Influenza in the Elderly." *Vaccine* 18 (16): 1686–89. https://doi.org/10.1016/S0264-410X(99)00507-1.

Weissman, Irving L., and Judith A. Shizuru. 2008. "The Origins of the Identification and Isolation of Hematopoietic Stem Cells, and Their Capability to Induce Donor-Specific Transplantation Tolerance and Treat Autoimmune Diseases." *Blood* 112 (9): 3543–53. https://doi.org/10.1182/blood-2008-08-078220.

Yamamoto, Ryo, Adam C. Wilkinson, Jun Ooehara, Xun Lan, Chen Yi Lai, Yusuke Nakauchi, Jonathan K. Pritchard, and Hiromitsu Nakauchi. 2018. "Large-Scale Clonal Analysis Resolves Aging of the Mouse Hematopoietic Stem Cell Compartment." *Cell Stem Cell* 22 (4): 600-607.e4. https://doi.org/10.1016/j.stem.2018.03.013.

Figure 1.

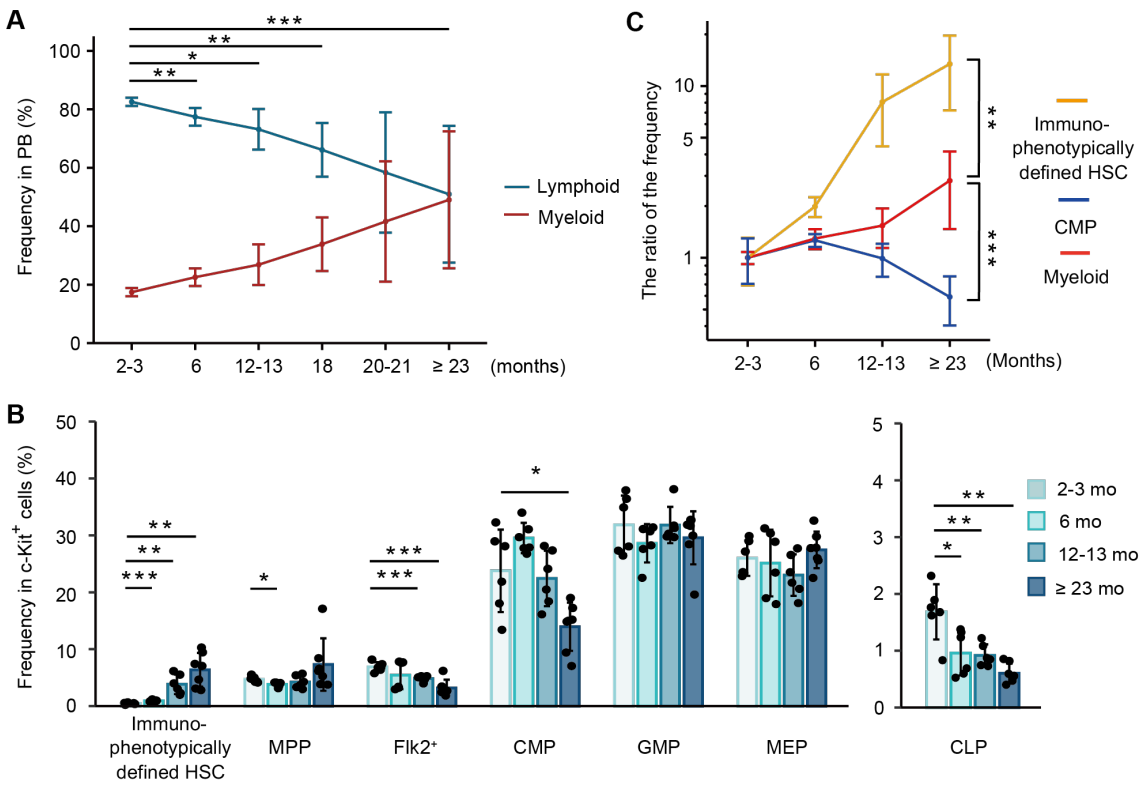

Figure 1. Comprehensive analysis of hematopoietic alternations with age shows a discrepancy of age-associated changes between peripheral blood and bone marrow

(A) Average frequency of myeloid cells (neutrophils, monocytes) and lymphoid cells (B cells, T cells, and NK cells) in PB at the age of 2-3 months (n = 6), 6 months (n = 6), 12-13 months (n = 6), 18 months (n = 6), 20-21 months (n = 5), ≥ 23 months (n = 16). Abbreviation: PB = Peripheral blood.

(B) Average frequency of immunophenotypically defined HSC and progenitor cells in BM of 2-3-month mice (n = 6), 6-month mice (n = 6), 12-13-month mice (n = 6), ≥ 23-month mice (n = 7).

(C) Age-associated changes of immunophenotypically defined HSC and myeloid differentiation components (CMP and myeloid cells in the PB). The ratio of aged to young

839 frequency was calculated as (the fraction frequency at each aged mice (%)) / (the average
840 fraction frequency at 2-3-month mice (%)). *$P < 0.05$. **$P < 0.01$. ***$P < 0.001$. Data
841 and error bars represent means ± standard deviation.
842
843
844
845
846
847
848
849
850
851
852
853
854
855
856
857
858
859
860
861
862

Figure 2.

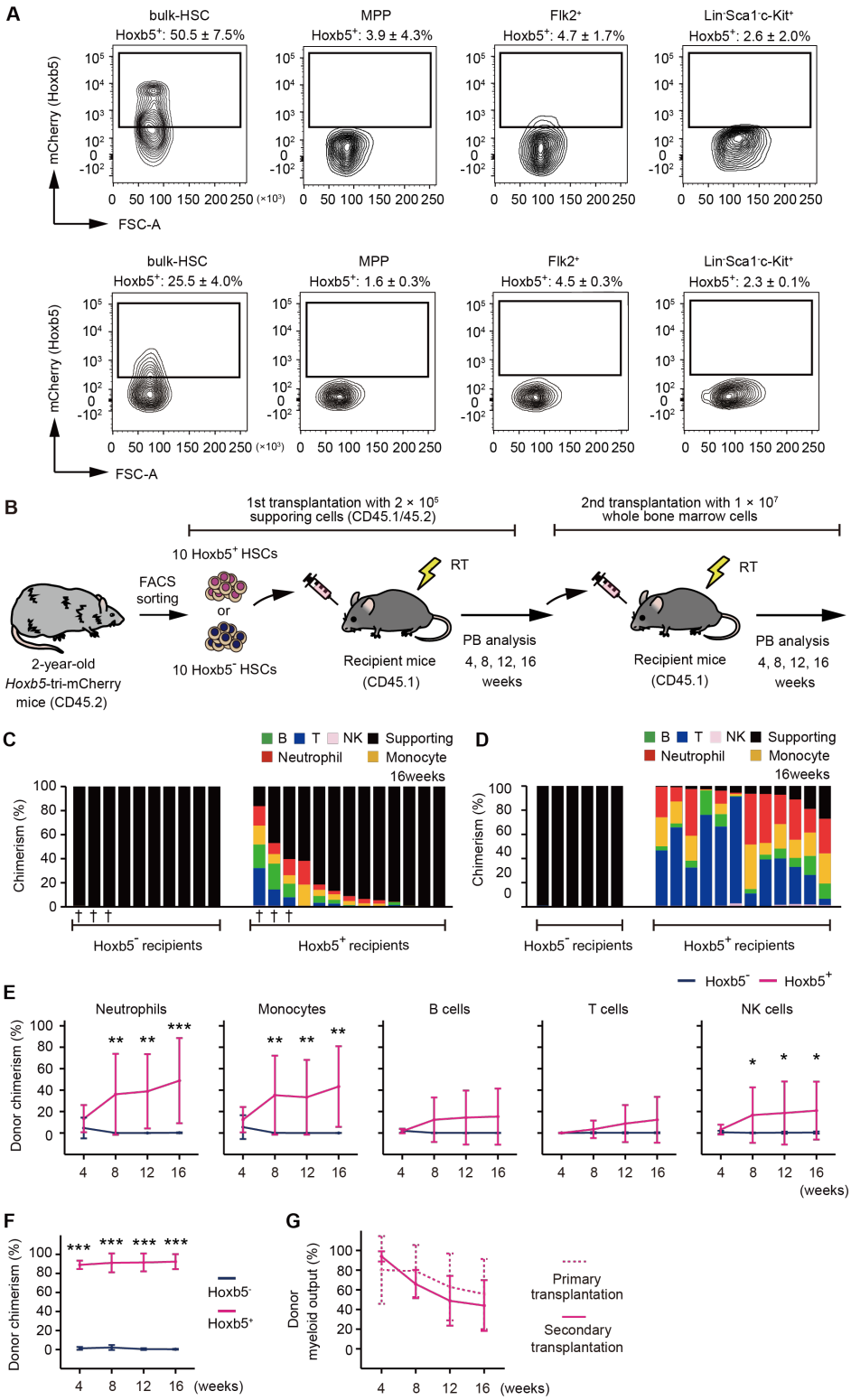
A
bulk-HSC
Hoxb5+: 50.5 ± 7.5%
MPP
Hoxb5+: 3.9 ± 4.3%
Flk2+
Hoxb5+: 4.7 ± 1.7%
Lin-Sca1-c-Kit+
Hoxb5+: 2.6 ± 2.0%
mCherry (Hoxb5)
FSC-A
bulk-HSC
Hoxb5+: 25.5 ± 4.0%
MPP
Hoxb5+: 1.6 ± 0.3%
Flk2+
Hoxb5+: 4.5 ± 0.3%
Lin-Sca1-c-Kit+
Hoxb5+: 2.3 ± 0.1%
B
1st transplantation with 2 × 10^5 supporing cells (CD45.1/45.2)
2nd transplantation with 1 × 10^7 whole bone marrow cells
10 Hoxb5+ HSCs
FACS sorting
or
10 Hoxb5- HSCs
2-year-old Hoxb5-tri-mCherry mice (CD45.2)
RT
Recipient mice (CD45.1)
PB analysis 4, 8, 12, 16 weeks
RT
Recipient mice (CD45.1)
PB analysis 4, 8, 12, 16 weeks
C
B T NK Supporting
Neutrophil Monocyte
16weeks
Chimerism (%)
Hoxb5- recipients
Hoxb5+ recipients
D
B T NK Supporting
Neutrophil Monocyte
16weeks
Chimerism (%)
Hoxb5- recipients
Hoxb5+ recipients
E
Hoxb5- Hoxb5+
Neutrophils
Monocytes
B cells
T cells
NK cells
Donor chimerism (%)
(weeks)
F
Donor chimerism (%)
Hoxb5-
Hoxb5+
(weeks)
G
Donor myeloid output (%)
Primary transplantation
Secondary transplantation
(weeks)

886 **Figure 2. The expansion of myeloid-biased clones was not observed in 2-year-old**
887 **LT-HSCs after their transplantation.**
888 (A) Hoxb5 reporter expression in bulk-HSC, MPP, Flk2$^+$, and Lin$^-$Sca1$^-$c-Kit$^+$
889 populations in the 2-year-old *Hoxb5*-tri-mCherry mice (Upper panel) and 3-month-old
890 *Hoxb5*-tri-mCherry mice (Lower panel). Values indicate the percentage of mCherry$^+$ cells
891 ± standard deviation in each fraction (n = 3).
892 (B) Experimental design to assess the long-term reconstitution ability of Hoxb5$^+$ HSCs or
893 Hoxb5$^-$ HSCs. Hoxb5$^+$ HSCs and Hoxb5$^-$ HSCs were isolated from 2-year-old CD45.2
894 *Hoxb5*-tri-mCherry mice and were transplanted into lethally irradiated CD45.1 recipient
895 mice with 2×10^5 supporting cells (Hoxb5$^+$ HSCs, n = 13; Hoxb5$^-$ HSCs, n = 10). For
896 secondary transplants, 1×10^7 whole BM cells were transferred from primary recipient
897 mice. Abbreviations: PB = Peripheral blood, RT = Radiation therapy.
898 (C) Percentage chimerism at 16 weeks after receiving ten aged Hoxb5$^-$ HSCs or ten aged
899 Hoxb5$^+$ HSCs. Each column represents an individual mouse.
900 (D) Percentage chimerism at 16 weeks after whole BM secondary transplantation. Donor
901 whole BM cells for secondary transplantation were taken from mice denoted by † in
902 Figure 2C.
903 (E) Kinetics of average donor chimerism in each PB fraction after primary
904 transplantation.
905 (F) Kinetics of average donor chimerism after secondary transplantation.
906 (G) Kinetics of average donor myeloid output (myeloid proportion in donor cells) in LT-
907 HSC recipient mice after primary and secondary transplantation. *$P < 0.05$. **$P < 0.01$.
908 ***$P < 0.001$. Data and error bars represent means ± standard deviation.
909

910 **Figure 3.**

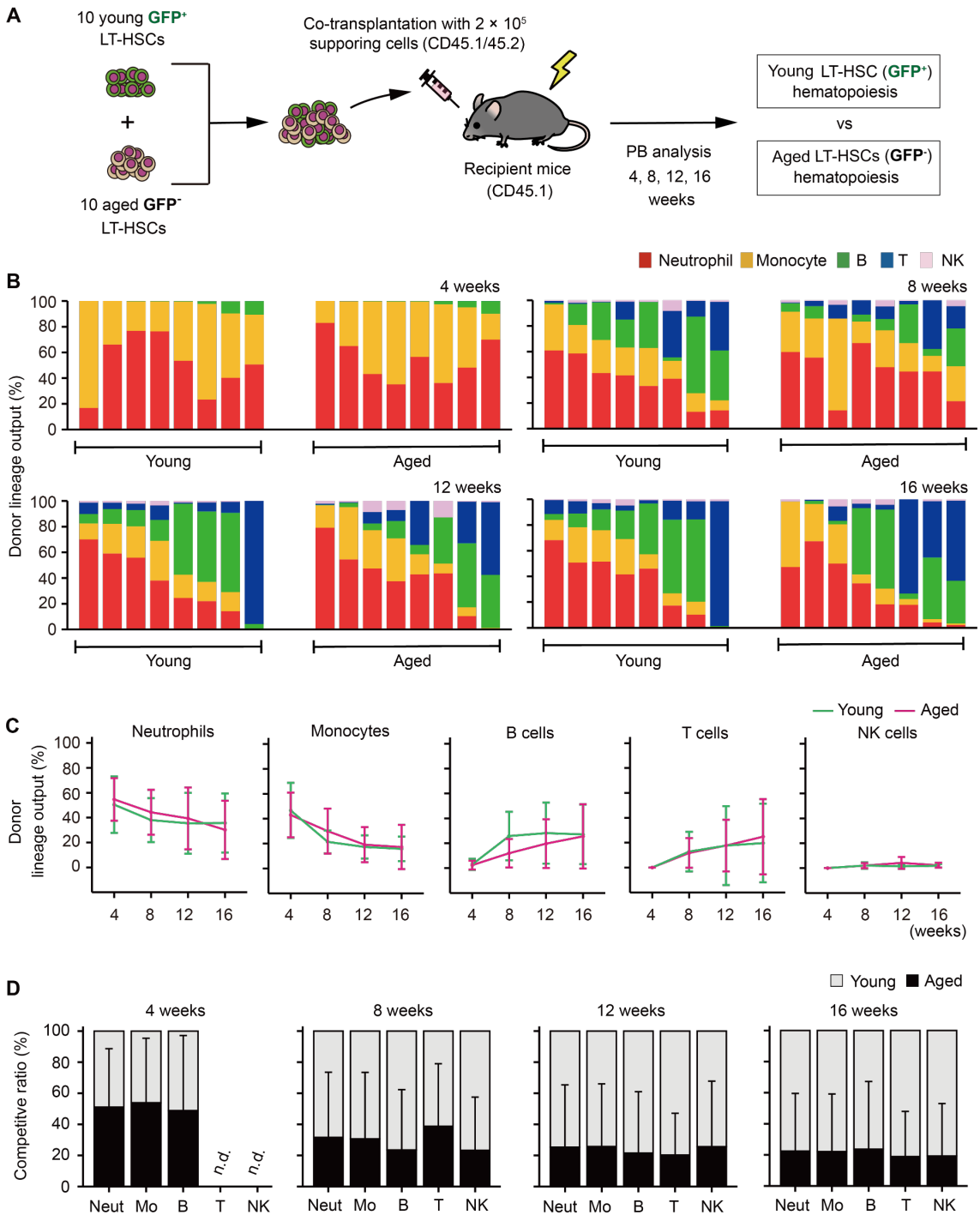

932 **Figure 3. Aged LT-HSCs show balanced hematopoiesis throughout life**

933 (A) Experimental design for competitive co-transplantation assay using young LT-HSCs
934 sorted from *Hoxb5*-tri-mCherry GFP mice and aged LT-HSCs sorted from *Hoxb5*-tri-
935 mCherry mice. Ten CD45.2^{+} young LT-HSCs and ten CD45.2^{+} aged LT-HSCs were
936 transplanted with 2×10^{5} CD45.1^{+}/CD45.2^{+} supporting cells into lethally irradiated
937 CD45.1^{+} recipient mice (n = 8).
938 (B) Lineage output of young or aged LT-HSCs at 4, 8, 12, 16 weeks after transplantation.
939 Each bar represents an individual mouse.
940 (C) Lineage output kinetics of young LT- HSCs or aged LT- HSCs at 4, 8, 12, 16 weeks
941 post-transplant.
942 (D) Competitive analysis of young LT-HSCs vs. aged LT-HSCs lineage output at 4, 8,
943 12, 16 weeks post-transplant. Competitive ratio was calculated as the proportion of young
944 LT-HSCs derived cells vs. aged LT- HSCs derived cells in each fraction. Abbreviations:
945 Neut = Neutrophils, Mo = Monocytes, B = B cells, T = T cells, and NK = NK cells. Data
946 and error bars represent means ± standard deviation. “n.d.” stands for “not detected.”
947
948
949
950
951
952
953
954
955
956

957 **Figure 4.**

958 A

959 Bone marrow analysis

960 Young or Aged

961 *Hoxb5*-tri-mCherry mice

bulk-HSC fraction

mCherry

FSC-A

LT-HSC (LT)

bulk-HSC (bulk)

ST-HSC (ST)

Library Preparation

Hisat2

Stringtie

EdgeR

Sequence & Analysis

962 B

963 Cluster dendrogram

964 Height

965 0.05

966 0.03

967 0.01

ST bulk LT LT bulk ST

Young Aged

968 C

INFLAMMATION

p53_PATHWAY

E2F_TARGET

AGING_SIGNATURE

Z score (TMM normalized read)

ST bulk LT

Young

Aged

969 D Myeloid gene sets relation

970 (A Sanjuan-Pla et al) (Pronk et al)

971 327 96 9 7 1 7 124

972 (SM Chambers et al)

973 E Lymphoid gene sets relation

974 (A Sanjuan-Pla et al) (Pronk et al)

975 348 101 12 2 17

976 (SM Chambers et al)

F Defined myeloid signature genes (111 genes)

bulk (Aged vs. Young) NES = 1.25 q = 0.067

ST (Aged vs. Young) NES = 1.05 q = 0.363

LT (Aged vs. Young) NES = 0.87 q = 0.752

Enrichment score

Aged enriched

Young enriched

G Defined lymphoid signature genes (103 genes)

bulk (Aged vs. Young) NES = 0.93 q = 0.639

ST (Aged vs. Young) NES = 0.87 q = 0.727

LT (Aged vs. Young) NES = 0.88 q = 0.720

977 **Figure 4. Myeloid-associated genes were not enriched in aged LT-HSCs compared**

978 **to their young counterparts**

979 (A) Experimental schematic for transcriptome analysis. LT-HSCs (n = 3), ST-HSCs (n =
980 3), and bulk-HSCs (n = 3) were sorted from young (2-3 months) or aged (23-25 months)
981 *Hoxb5*-tri-mCherry mice, after which each RNA was harvested for RNA sequencing.
982 (B) Hierarchical clustering dendrogram of whole transcriptomes using Spearman distance
983 and the Ward clustering algorithm.
984 (C) Violin plots showing normalized gene expression levels for each gene set in young
985 and aged LT-HSCs, ST-HSCs, and bulk-HSCs. Expression values for each gene were
986 standardized independently by applying *Z* score transformation.
987 (D, E) Venn diagram showing the overlap of genes between three myeloid signature gene
988 sets, and lymphoid signature gene sets (A Sanjuan-Pla et al., 2013, Pronk et al., 2007, SM
989 Chambers et al., 2007).
990 (F, G) Signature enrichment plots from GSEA analysis using defined myeloid and
991 lymphoid signature gene sets that overlapped in the three gene sets. Values indicated on
992 individual plots are the normalized Enrichment Score (NES) and q-value of enrichment.
993 ***$P < 0.001$.
994
995
996
997
998
999
1000
1001
1002

1003 **Figure 5.**

1004 1005 1006 1007 1008 1009 1010 1011 1012 1013 1014 1015

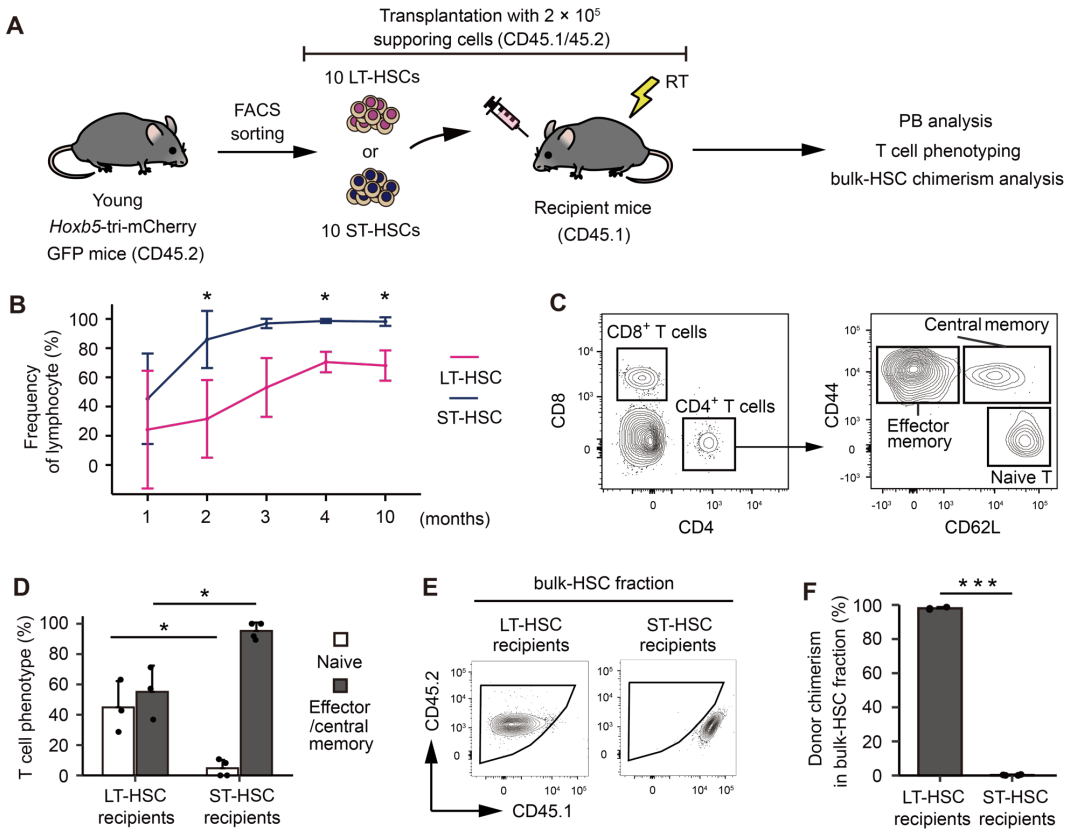

1016

1017 **Figure 5. The memory-type lymphocytes in the peripheral blood make it look as if**

1018 **ST-HSCs are lymphoid-biased HSCs**

1019 (A) Experimental design for assessing the lineage output of young LT-HSCs or ST-HSCs.

1020 Ten LT-HSCs, or ten ST-HSCs were isolated from 2-month-old CD45.2 *Hoxb5*-tri-

1021 mCherry GFP mice and were transplanted into lethally irradiated CD45.1 recipient mice

1022 with 2×10^5 supporting cells (LT-HSCs, $n = 3$; ST-HSCs, $n = 4$).

1023 (B) Kinetics of average frequency of lymphoid cells (B cells, T cells, and NK cells) in

1024 donor fraction after LT-HSCs or ST-HSCs transplantation.

1025 (C) Gating scheme to identify memory (Central and effector) T cells and naive T cells in

1026 the PB after excluding doublets, dead cells, and non-donor cells.

1027 (D) Percentage of memory (Central and effector) T cells and naive T cells in donor $CD4^+$
1028 fraction 10 months after LT-HSC or ST-HSC transplantation.
1029 (E) Gating scheme to identify donor cells in bulk-HSC fraction in bone marrow analysis.
1030 (F) Donor chimerism in bulk-HSC fraction 12 months after LT-HSCs or ST-HSCs
1031 transplantation. *$P < 0.05$. ***$P < 0.001$. Data and error bars represent means ± standard
1032 deviation.
1033
1034
1035
1036
1037
1038
1039
1040
1041
1042
1043
1044
1045
1046
1047
1048
1049
1050

1051 **Figure 6.**

1052 1053 1054 1055 1056 1057 1058 1059 1060 1061 1062 1063 1064 1065 1066 1067 1068 1069

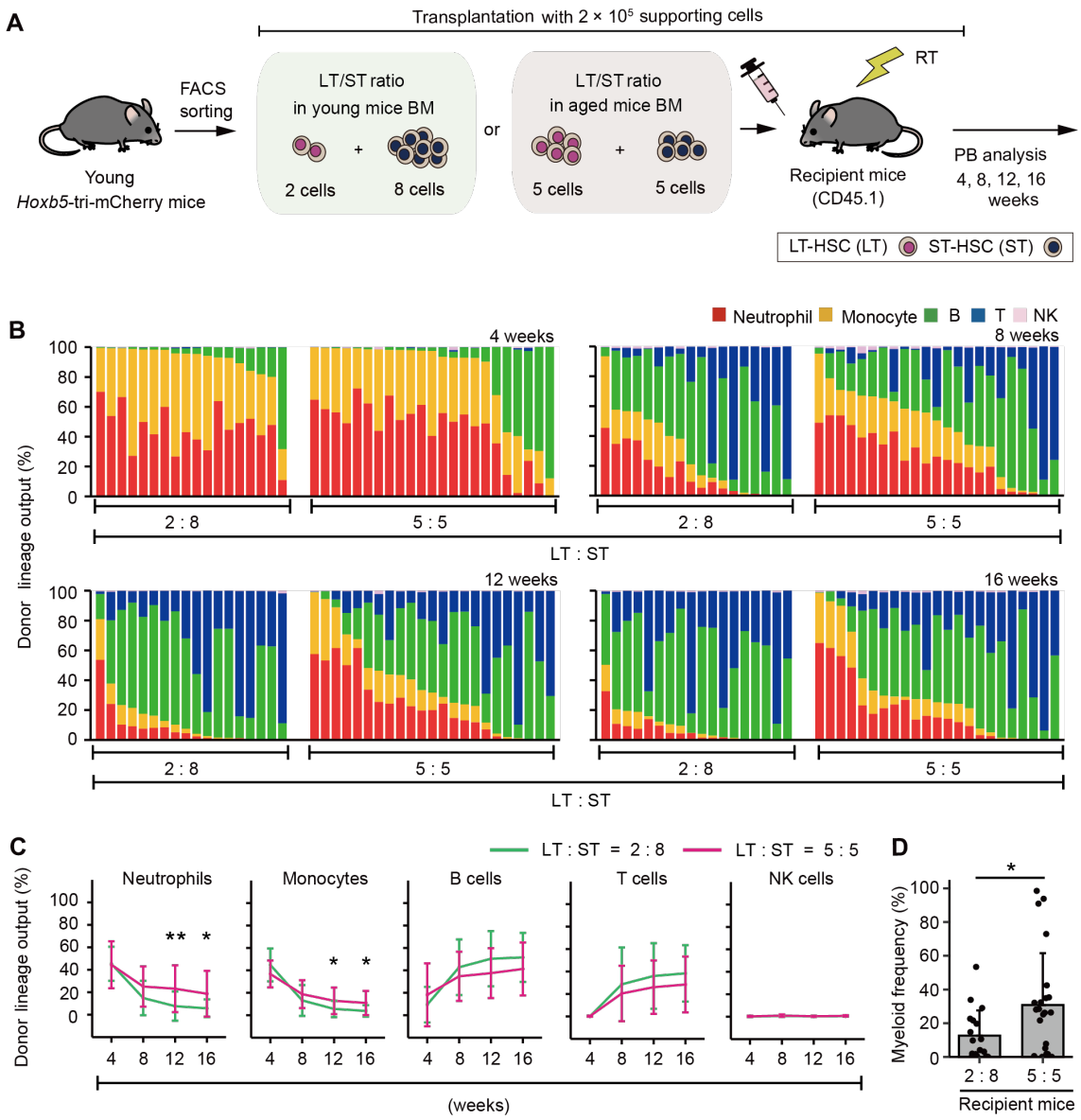

Figure 6. Hematopoiesis after transplantation inclined either toward myeloid or lymphoid cell production by artificially changing the ratio of LT-HSC/ST-HSC

(A) Experimental design for the transplantation of 2-3-month-old LT-HSCs and ST-HSCs in a 2:8 ratio (the same ratio as in young mice BM) or 5:5 ratio (the same ratio as in aged mice BM). Donor cells were transplanted with 2 × 10^5 CD45.1$^+$/CD45.2$^+$

1075 supporting cells into lethally irradiated CD45.1^{+} recipient mice (2:8 ratio, n = 18; 5:5
1076 ratio, n = 23).
1077 (B) Donor lineage output of young LT-HSCs and ST-HSCs transplanted either in a 2:8
1078 ratio or a 5:5 ratio at 4, 8, 12, 16 weeks post-transplant. Each bar represents an individual
1079 mouse.
1080 (C) Kinetics of average lineage output of young LT-HSCs and ST-HSCs in a 2:8 ratio or
1081 a 5:5 ratio at 4, 8, 12, 16 weeks post-transplant.
1082 (D) Frequency of myeloid cells in donor cell fraction. *$P < 0.05$. **$P < 0.01$. Error bars
1083 represent standard deviation. Data represent two independent experiments.
1084
1085
1086
1087
1088
1089
1090
1091
1092
1093
1094
1095
1096
1097
1098

Figure 7.

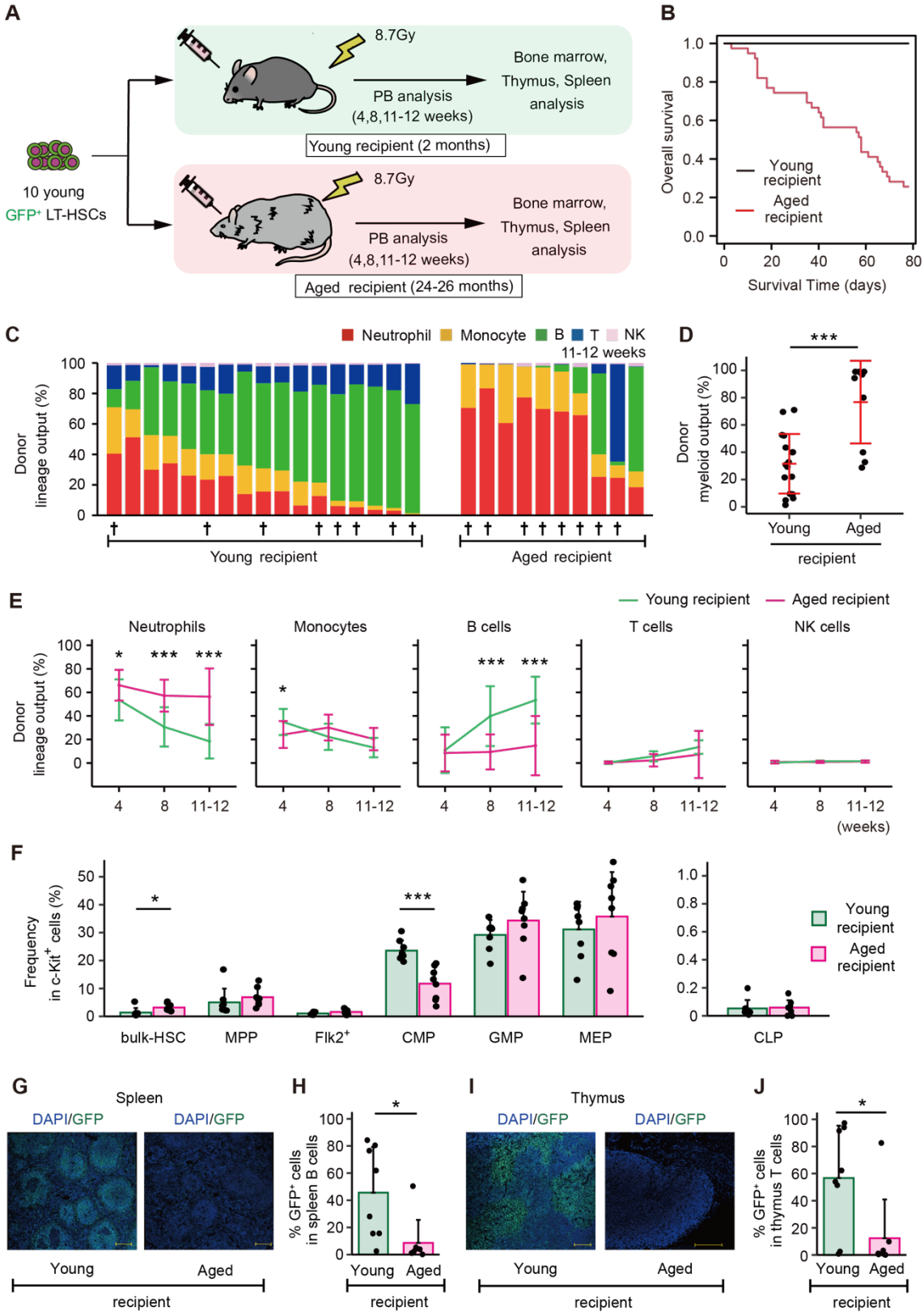
A
8.7Gy
Bone marrow, Thymus, Spleen analysis
PB analysis (4,8,11-12 weeks)
Young recipient (2 months)
10 young GFP+ LT-HSCs
8.7Gy
Bone marrow, Thymus, Spleen analysis
PB analysis (4,8,11-12 weeks)
Aged recipient (24-26 months)
B
Overall survival
Young recipient
Aged recipient
Survival Time (days)
C
Neutrophil Monocyte B T NK
11-12 weeks
Donor lineage output (%)
Young recipient
Aged recipient
D
***
Donor myeloid output (%)
Young
Aged
recipient
E
Young recipient
Aged recipient
Neutrophils
Monocytes
B cells
T cells
NK cells
Donor lineage output (%)
(weeks)
F
Frequency in c-Kit+ cells (%)
bulk-HSC
MPP
Flk2+
CMP
GMP
MEP
CLP
Young recipient
Aged recipient
G
Spleen
DAPI/GFP
DAPI/GFP
Young
Aged
recipient
H
% GFP+ cells in spleen B cells
Young
Aged
recipient
I
Thymus
DAPI/GFP
DAPI/GFP
Young
Aged
recipient
J
% GFP+ cells in thymus T cells
Young
Aged
recipient

1123 **Figure 7. Age-associated physiological changes drive differentiation of LT-HSCs**
1124 **toward myeloid cells**

1125 (A) Experimental design for assessing the impact of age-associated physiological changes
1126 on differentiation of LT-HSCs. Ten GFP^+ LT-HSCs sorted from young (2-3 months)
1127 *Hoxb5*-tri-mCherry GFP mice, were transplanted with 2×10^5 $CD45.1^+/CD45.2^+$
1128 supporting cells into lethally irradiated young or aged recipient mice. We defined donor
1129 cells as GFP^+ cells and supporting cells as $CD45.1^+/CD45.2^+$ cells.

1130 (B) Survival rate of recipient mice in each group.

1131 (C) Donor lineage output in young or aged recipient mice 11-12 weeks after transplanting
1132 young LT-HSCs (young recipient, n = 17; aged recipient, n = 10).

1133 (D) Myeloid output (Frequency of donor myeloid cells in donor fraction) in young or
1134 aged recipient mice 11-12 weeks after transplantation.

1135 (E) Kinetics of lineage output from donor LT-HSCs in young or aged recipient mice 4, 8,
1136 11-12 weeks after transplantation.

1137 (F) Average frequency of donor bulk-HSC and progenitor cells in donor c-Kit^+ cells in
1138 BM (young recipient, n = 8; aged recipient, n = 8). BM samples were taken from mice
1139 denoted by † in Figure 7C.

1140 (G) Representative immunofluorescence images of frozen spleen sections derived from
1141 young or aged recipient mice. Green: donor cells (GFP fluorescence); blue: DNA (DAPI);
1142 Scale bar: 200 μm.

1143 (H) Frequency of donor cells in spleen B cells of young or aged recipient mice (young
1144 recipient, n = 8; aged recipient, n = 8). Spleens are taken from mice denoted by † in Figure
1145 7C.

1146 (I) Representative immunofluorescence images of frozen thymus sections derived from
1147 young or aged recipient mice. Green: donor cells (GFP fluorescence); blue: DNA (DAPI);
1148 Scale bar: 200 μm.
1149 (J) Frequency of donor cells in thymus T cells of young or aged recipient mice (young
1150 recipient, $n = 8$; aged recipient, $n = 8$). Thymi are taken from mice denoted by † in Figure
1151 7C. *$P < 0.05$. ***$P < 0.001$. Error bars represent standard deviation. Data represent two
1152 independent experiments.
1153
1154
1155
1156
1157
1158
1159
1160
1161
1162
1163
1164
1165
1166
1167
1168
1169

1170 **Figure 8.**

1171 Self-renewal heterogeneity model

1172 HSC differentiation

1173 LT-HSC

1174 Memory lymphocyte

1175 Myeloid cells

1176 De novo lymphocyte

Unbiased hematopoiesis

ST-HSC

Rapid turn over

Residual lymphocyte in PB

1177

1178

1179 In vivo differentiation

1180 Young

bulk-HSC fraction

Aged

bulk-HSC fraction

1181 Alternation of LT-HSC/ST-HSC ratio

1182

1183 Thymus, Spleen function

1184

1185

1186 Balanced hematopoiesis

Myeloid biased hematopoiesis

1187

1188 **Figure 8.** Our new model: **Self-renewal heterogeneity model**. It has been thought that

1189 there were myeloid (My-) or lymphoid biased (Ly-) HSCs, and that clonal selection of

1190 My-HSCs caused age-associated myeloid biased hematopoiesis. However, in our model,

1191 LT-HSCs represent unbiased hematopoiesis throughout life. ST-HSCs lose their

1192 hematopoietic ability within a short period and memory-type lymphocytes remains in the

1193 PB after ST-HSC transplantation. These remaining memory-type lymphocytes make it

look as if ST-HSCs are lymphoid-biased (The upper section). As a result, the age-associated relative decrease of ST-HSCs in bulk-HSC fraction causes myeloid biased hematopoiesis with age. Additionally, the blockage of lymphoid differentiation at spleen and thymus accelerates further myeloid biased hematopoiesis in aged mice (The lower section).